Quench Protection of Fusillo Subscale Curved CCT Magnet

M. Wozniak, A. Haziot, F. J. Mangiarotti, E. Ravaioli, R. Ferriere, J. G. Valenzuela, A. P. Foussat, G. Kirby, and A. Verweij

***Abstract*—The Fusillo project at CERN aims to design and build a demonstrator magnet with multi-harmonic corrected fields in a 90° curved CCT magnet. In the first stage, a subscale magnet is built with 30° bending, about 1/30 of the demonstrator conductor length, and increased current to reach coil stresses equivalent to the demonstrator. The subscale magnet enables qualification of the technology developments, fabrication methods, winding and assembly procedures, and magnetic and quench protection design and measurement setups. The subscale magnet comprises two tilted solenoids with an opposite inclination on curved aluminium formers. Each solenoid has two channel turns with 70 Nb-Ti/Cu wires. The magnet is protected by an active quench detection with energy extraction (EE). EE causes current decay, which induces eddy currents in the formers. As a result, the differential inductance of the magnet is reduced, and the formers heat up, with the potential to strongly influence the quench behaviour of the windings. Calculation of the eddy currents and heat propagation in the formers with simultaneous quench propagation in the magnet windings requires a three-dimensional (3D) simulation. A cooperative simulation approach has been developed to simulate transients in this magnet. It involves two software tools developed at CERN as part of the STEAM framework: a finite element-based tool called FiQuS and a finite difference-based tool called LEDET. FiQuS calculates eddy currents in the formers and the temperature of the formers, whereas LEDET calculates windings' temperature, current and voltage. This approach enables a 3D quench simulation with great geometrical detail while maintaining reasonable computational cost. The simulation results are compared to measurement results from the forced EE. The agreement between the measurements and simulations is presented, and the key factors that affect magnet quench behaviour are identified.**

***Index Terms*—Computer-aided engineering, finite difference methods, finite element method, superconducting magnets, quench protection.**

I. Introduction

RECENT progress in magnet design tools [1], [2] made it relatively straightforward to design Curved Canted Cosine Theta (CCCT) magnets with the modulation of the winding path required to balance out the field harmonics resulting from the curvature. As a result, magnet windings take elaborate shapes, and with Computer Numeric Control (CNC) machining, the complex channels for placing the windings in the formers can be manufactured. For many applications, increasing the number of turns is preferred in order not to exceed the magnet current above a couple of hundred amperes. Winding the high number of turns can be simplified by utilizing a cable consisting of twisted and insulated strands connected in series [3].

The Fusillo project at CERN greatly benefits from these advances and solutions and is focused on developing the technology for CCCT magnets [3]. The project is complementary to [4]. Various Fusillo subscale CCCT magnets will be constructed to enable qualification of the technology developments, fabrication methods, winding and assembly procedures, and magnetic and quench protection design and measurement setups. The first Fusillo subscale magnet (FSM1) has two layers with two-channel turns per layer and 70 wire turns in the channel. The forces on the windings match the full-scale magnet, thanks to operation at a higher current. The quench protection of FSM1 is not challenging due to the availability of an Energy Extraction (EE) system at the CERN magnet test facility.

Many quench-related measurements have been performed on the FSM1. An in-depth analysis of these results is in progress, and here, we only focus on the initial five forced energy extractions. These measurements are particularly relevant as they constitute the first reference to validate the ongoing effort of developing CCCT quench simulation capability at CERN.

Due to the complex shape of the coils, the formers, and the shell of the FSM1, it is necessary to perform simulations in 3-dimensions (3D). To account for the eddy currents in the formers and the shell, a finite element simulation approach is applied. Due to the relatively high number of turns (70) in the channel, an efficient approach for heat diffusion in the windings needs to be used, and the finite difference method is employed. For these tasks, the Finite Element Quench Simulator (FiQuS) [5], [6], [7] and Lumped-Element Dynamic Electro-Thermal (LEDET) [8], [9], [10] tools are used. In a cooperative simulation (co-simulation) [11] with data exchange between the tools. This approach has been developed as part of the STEAM (Simulation of Transient Effects in Accelerator Magnets) framework [12].

Previous works on such type of simulation include the incorporation of the 3D eddy currents in the aluminium structures in the simulation presented in [13]; however, there is no effect of a quench in the windings due to omitting heat diffusions in them. Furthermore, the simulation approach as in [14] omits the temperature gradient along the superconducting wires, rendering the heat diffusion in the winding as 2-dimensional (2D). Additionally, the approach does not include any calculation of the eddy current in the conducting structures as the formers, as the simulated magnets are made with insulating material (G10). Another approach was published in [15] with 2D heat diffusion in the windings and the conducting structures

Manuscript received 26 September 2023; revised 23 November 2023 and 24 December 2023; accepted 11 January 2024. Date of publication 17 January 2024; date of current version 14 February 2024. *(Corresponding author: M. Wozniak.)*

The authors are with CERN, 1211 Meyrin, Switzerland (e-mail: mariusz.wozniak@cern.ch).

Color versions of one or more figures in this article are available at https://doi.org/10.1109/TASC.2024.3355358.

Digital Object Identifier 10.1109/TASC.2024.3355358

TABLE I
KEY PARAMETERS OF THE FSM1 [3]

Parameter	Subscale #1	Unit
Free aperture	236	mm
Curvature radius	1.0	m
Magnetic bend/length	30 / 0.53	° / m
Bore/peak field at I_{nom}	0.48 / 2.2	T
Nominal current I_{nom}	540	A
Measured inductance	38.75	mH
Formers and shell material	EN AW-6082 T6	-
Formers and shell RRR	4.14	-
# channel turns per layer	2	-
# conductors in channel	70	-
Total weight	310	kg

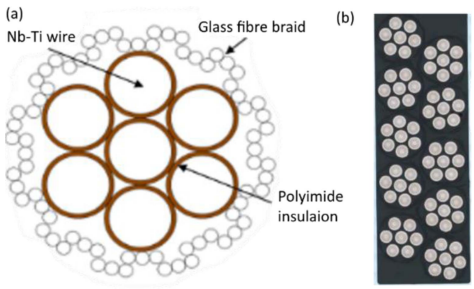

Fig. 1. (a) Schematic of the rope cable. (b) Cross-sections of the groove with the winding consisting of 10 rope cables with 6-around-1 Nb-Ti wires [3].

coupled with an electrical circuit model using self- and mutual-inductances between the subsequent model parts.

The co-simulation approach in this contribution allows accounting for the 3D eddy currents in the conducting structures and 3D heat diffusion in the windings and conducting structures. This renders it the most comprehensive within the literature.

II. MAGNET AND MEASUREMENT SETUP

The FSM1 details are given in [3]. Selected key parameters are shown in Table I. The coils are wound with a so-called rope cable. The cable is composed of 7 round Nb-Ti/Cu superconducting (SC) strands, 825 µm bare diameter with a Cu:SC ratio of 1.95:1, a Cu RRR of at least 150, and a filament twist-pitch length of 15 mm. This is the strand used in the outer layer of the main bending dipoles (MB) and in the main quadrupoles (MQ) of the Large Hadron Collider. Strand insulation is added, consisting of polyimide tape wrapped in two layers of 25 µm with 50% overlap and a total thickness of 76 µm. Seven of such insulated strands are twisted in 6-around-1 configuration to form a cable. After winding, the strands are electrically connected in series by splicing [3]. Additional cable insulation of S2 glass fibre braid is added, with a nominal thickness of 100 µm. The insulation provides a relatively thick (176 µm) insulation of the strands to the formers, which is beneficial for the insulation breakdown voltage level. In addition, the glass fibre braid of the cables is impregnated with the resin (see Fig. 1 [3]) and forms a mechanically beneficial composite structure in the channel.

The quench detection settings do not affect the forced EE results presented here. The FSM1 was powered in the circuit with the schematic in Fig. 2. The power converter (PC) output

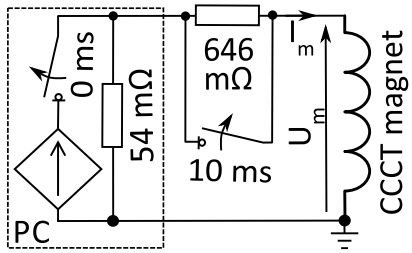

Fig. 2. Schematic of the magnet circuit including power converter (PC), energy extraction system, and the CCCT magnet.

stage changes to a high impedance state at 0 ms and results in the magnet current commuting to the PC's internal crowbar resistor of 54 mΩ. After 10 ms, the EE switch is opened, introducing 646 mΩ of EE resistance in the discharge circuit. The forced EEs were performed at 100, 220, 340, 460, and 580 A. All measurements were performed at a temperature of 4.2 K.

III. SIMULATIONS SETUP

FiQuS and LEDET tools are used in the co-simulation, with Python scripts maintaining and controlling communication, data exchange, and convergence [11].

A. Finite Element Tool

The open-source FiQuS is coded in Python [16] and, with the help of Gmsh [17], [18] and GetDP [19], [20] performs geometry generation, meshing, solving, and post-processing.

The magnet design enters the simulations as two sets of conductor files [21] for windings and STEP [22] files for the geometry of the formers and shell. The air region needed for the magnetoquasistatic solution is parametrically generated and modeled as a cylinder with a 1.4 m diameter around the magnet center.

The windings geometry was adapted to add so-called terminals extending to the flat ends of the cylindrical air region. The intersection of the terminals' geometry and the air boundary defines the surfaces for applying the current to power the magnet. These terminals add magnetic field and inductance contributions. As a result, the simulated magnet inductance is 39.22 mH, which overestimates the measured inductance (Table I) by about 1.2%.

The formers have an increased outer radius to compensate for the air gap between formers or between the former and the shell, following the approach as in [11]. The shell is modelled as a single body, i.e., neglecting its horizontal split. The extremity flanges are neglected in the model. However, the cut-outs for the layer jump and the joint box in the outer former and the shell are included (see exploded view in Fig. 6 of [3] for details).

As detailed in [11], the elements of the above-described geometry are subjected to a series of Boolean operations to create a conformal geometry with no air gaps between the conductors and the channels of the formers as well as between the formers and the shell.

This conformal geometry greatly simplifies the meshing of the FSM1 model. The mesh used in the simulations included 180 k and 96 k tetrahedra for the regions used in the magnetoquasistatic and thermal calculations, respectively.

The finite element solution consists of coupled magneto-quasistatic and thermal diffusion models, including a special treatment of the collapsed air gaps [11]. In the thermal problem,

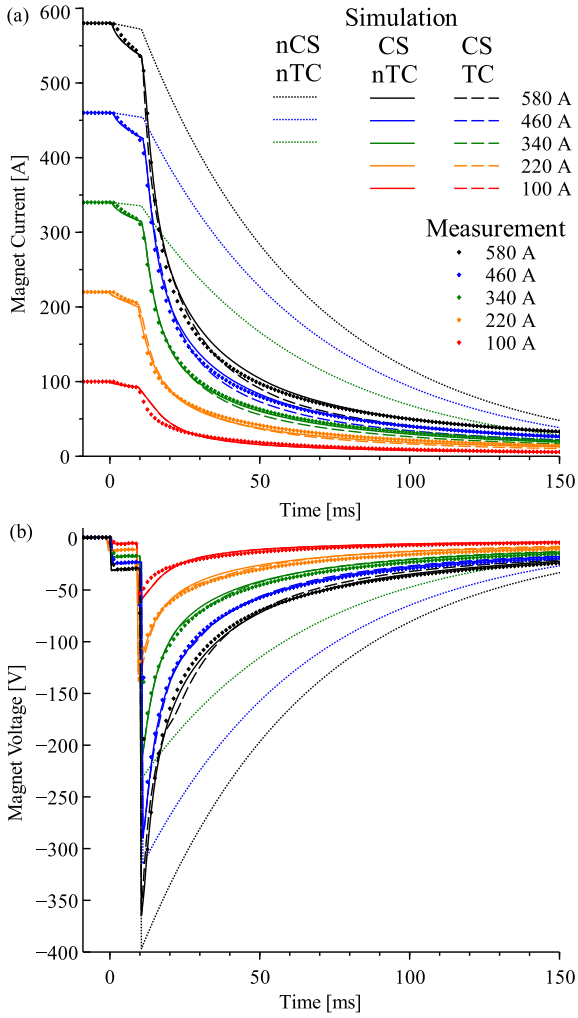

Fig. 3. Comparison of measured and simulated: (a) Currents and (b) voltages versus time for 5 initial extraction current levels. The no co-simulation (nCS) case is with constant inductance (L = const.), whereas co-simulation (CS) case is with differential inductance ($L \neq$const.) and iterative approach. For nCS case, only the three highest currents are shown for clarity. Simulations when thermal connection (TC) or no thermal connection (nTC) were used from the formers to the windings.

there is neither helium cooling of the formers or shell nor a heat exchange between them, i.e., each part is considered adiabatic. The formers and shell electrical and thermal conductivity and heat capacity are temperature dependent [23] and an RRR of 4.14 for the 6082 T6 aluminum alloy was used [24].

B. Finite Difference Tool

LEDET is coded in MATLAB [25] with a semi-implicit transient thermal solver that accounts for 3D heat diffusion along and between the windings as well as Joule and Inter-Filament Coupling Loss (IFCL) [8], [9].

The channels in the formers have 70 strands in the form of 10 rope cables. The strands are simulated as straight (i.e., non-twisted conductors). The polyimide strand insulation and the glass fibre cable insulation can be independently modeled in LEDET. The cable insulation thickness was increased because the strands are twisted and have increased distance from each other and the channel walls. Appropriate thermal connections along the width and height direction were specified to capture

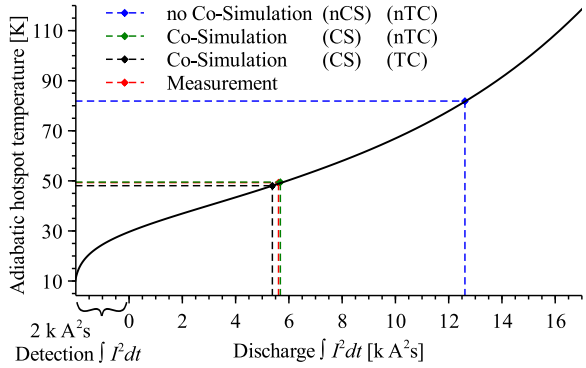

Fig. 4. Calculated at 0 T adiabatic hotspot temperature for the magnet wire (with Cu RRR = 150) vs discharge current integral. The measured and simulated quench discharge quench integrals correspond to the 580 A forced extraction. For detection, 2 k A^2s was assumed, corresponding to the total quench detection and validation time of 6 ms.

the complex heat exchange patterns between the strands in the cable and between the cables and the formers. These thermal connections use equivalent thicknesses and series connections of insulation layers involved.

IV. Results and Discussion

A full set of measured data at 5 different extraction currents is shown in Fig. 3 and compared to three simulation cases.

The no-co-simulation (nCS) case is with a fixed static inductance. This case corresponds to omitting the effects of the conducting structures and subsequently having no thermal connection (nTC) from the formers to the windings. With such a setup, the simulated currents decay exponentially with a time constant inversely proportional to the sum of the circuit and the magnet resistances. With such current and field change rates, the IFCL does not cause enough heating to quench the magnet, so the magnet resistance remains zero. The results of this simulation case do not match measured currents and voltages.

The other two simulation cases in Fig. 3 were calculated using the same co-simulation (CS) approach with updates to the differential inductance ($L \neq$const.) during iterations and solving for the heat diffusion in the conducting structures. The cases differ by having thermal connections (TC) or no thermal connections (nTC) from the formers to the windings. In the nTC case, the temperature of the formers does not affect the temperature of the windings as the thermal connections were disabled. The results of co-simulations match the measured curves well, and the differences between the TC and nTC cases are small. For 580 A discharge, a characteristic kink (around 20 ms) in the simulated voltage signal is present, corresponding to the onset of the quench-back of the windings. The measured voltage signal lacks such a feature, suggesting that no quench-back occurred in the FSM1 at 580 A (and, of course, neither at the lower currents, as shown in Fig. 3).

With the heat exchange between the formers and the windings disabled (nTC) in the simulation, the results match the measured results slightly better, although the difference is small, particularly for lower initial extraction currents, and the 100 A cases are the same. With the thermal connection enabled (TC) the simulations overestimate the thermal diffusion between the windings and the former. A possible explanation is that the windings are somewhat separated from the formers due to the difference in thermal contraction between them. This would

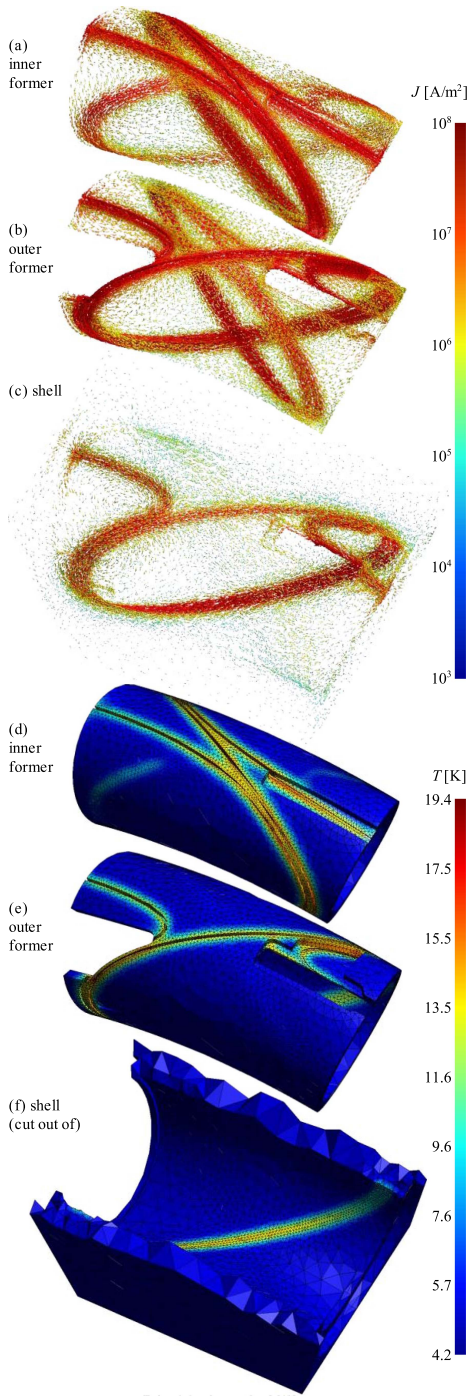

Fig. 5. (a)–(c) Simulated eddy current density and (d)–(f) temperature of the formers and shell, all at $t = 13.9$ ms. Eddy current density is shown in (a)–(c) with arrows to visualize the current flow direction. Part of the shell is shown in (f) to visualize the temperature in the bore. All to the same scale.

worsen the thermal contact and in addition, cause the presence of helium in the gap and add a local heat capacity, potentially resulting in no quench-back. Further quantification of this effect will be conducted with a full set of measurement results, where heaters on the formers were used to initiate the quench of the windings.

The measured discharge quench integral (QI) for 580 A forced extraction is 5.61 k A^2s. The corresponding QI calculated using the co-simulation results are 5.68 and 5.38 k A^2s for the nTC and TC cases, respectively. These correspond to the difference of 1.2 and 4.1%, compared to the measurements. The QI calculated for the no co-simulation case is 12.61 k A^2s, overestimating the measured QI by 225%. These results show that the eddy currents in the formers and the shell substantially affect the quench behaviour of the FSM1, and their influence on the differential inductance must be included in the simulations to avoid substantial overestimation of the discharge QI.

These QIs correspond to the adiabatic winding hot spot temperature for the Nb-Ti strand of the FSM1 (Fig. 4). Assuming 2 k A^2s for detection QI, the measured discharge QI corresponds to 49.3 K, and co-simulations discharge QIs correspond to 49.5 and 48.1 K for the nTC and TC case, respectively. The discharge QI from the no co-simulation corresponds to 81.9 K, corresponding to an overestimation of the adiabatic hot spot temperature by about 1.7 times.

The measured and co-simulated adiabatic hot spot temperature below 50 K confirms that the quench protection of the FSM1 is not particularly challenging as energy extraction can be used.

With the confidence that the co-simulation results for the nTC case match the measurements, it is interesting to visualize the eddy current density in the formers and shell with the temperature distribution developed due to the Joule heating (Fig. 5).

The eddy current pattern in the formers resembles the winding shape, and the current density is the highest close to the channels. The shell has no machined channels; however, the induced currents resemble the outer winding shape. The cut-outs, particularly in the outer former for the layer jump and the joint box, affect the current distribution.

The temperature distribution is non-uniform, with the 'hot spots' clearly visible and corresponding to the locations where the eddy current density and associated power density are the highest.

The total co-simulation time on a typical desktop computer was about 3 h, and 5 iterations were sufficient for the co-simulation to converge with a criterion based on the magnet current, i.e., $\forall t$: $|I_{\mathrm{iter.N}}(t) - I_{\mathrm{iter.N\text{-}1}}(t)| < 1.5$ A.

V. Conclusion

The recently developed co-simulation between the finite elements and finite difference tools of the STEAM framework has been used to simulate transients in the first Fusillo subscale CCCT magnet. An initial set of 5 measured forced energy extractions has been used to validate this simulation approach. A good degree of agreement between measurement and simulation was achieved.

The results provide valuable insights into the quench behavior of the CCCT magnets, particularly their differential inductance, eddy current patterns, and formers temperature distribution, which is key for predicting the location and timing of quench-back in the windings. The sensitivity of the co-simulation results to the uncertainty of the thermal resistance between the formers and the winding was demonstrated. The thermal resistance uncertainty remains a key obstacle to achieving a better predictive ability in simulating the quench-back.

Further measurements and simulation comparisons are in progress and will further improve the predictive quench simulation ability for the CCCT magnets at CERN.

REFERENCES

[1] ROXIE Users Workshop and ROXIE23 Launch, 2023. Accessed: Feb. 5, 2024. [Online]. Available: https://indico.cern.ch/event/1318061/

[2] M. Liebsch and S. Russenschuck, "A CAD engine based on the differential geometry of the frenet frame," *IEEE Trans. Appl. Supercond.*, vol. 34, no. 5, Aug. 2024, Art. no. 4900205, doi: 10.1109/TASC.2023.3338167.

[3] A. Haziot et al., "Curved-canted-cosine-theta (CCCT) dipole prototype development at CERN," *IEEE Trans. Appl. Supercond.*, early access, Jan. 12, 2024, doi: 10.1109/TASC.2024.3353149.

[4] G. Kirby et al., "Superconducting curved canted–cosine–theta (CCT) for the HIE-ISOLDE recoil separator ring at CERN," *IEEE Trans. Appl. Supercond.*, vol. 32, no. 6, Sep. 2022, Art. no. 4004105, doi: 10.1109/TASC.2022.3158332.

[5] A. Vitrano, M. Wozniak, E. Schnaubelt, T. Mulder, E. Ravaioli, and A. Verweij, "An open-source finite element quench simulation tool for superconducting magnets," *IEEE Trans. Appl. Supercond.*, vol. 33, no. 5, Aug. 2023, Art. no. 4702006, doi: 10.1109/TASC.2023.3259332.

[6] M. Wozniak, E. Ravaioli, and A. Verweij, "Fast quench propagation conductor for protecting canted cos-theta magnets," *IEEE Trans. Appl. Supercond.*, vol. 33, no. 5, Aug. 2023, Art. no. 4701705, doi: 10.1109/TASC.2023.3247997.

[7] STEAM FiQuS, 2022. Accessed: Feb. 5, 2024. [Online]. Available: https://cern.ch//fiqus

[8] E. Ravaioli, B. Auchmann, M. Maciejewski, H. H. J. T. Kate, and A. Verweij, "Lumped-element dynamic electro-thermal model of a superconducting magnet," *Cryogenics*, vol. 80, pp. 346–356, Dec. 2016, doi: 10.1016/j.cryogenics.2016.04.004.

[9] E. Ravaioli, O. T. Arnegaard, A. Verweij, and M. Wozniak, "Quench transient simulation in a self-protected magnet with a 3-D finite-difference scheme," *IEEE Trans. Appl. Supercond.*, vol. 32, no. 6, Sep. 2022, Art. no. 4005205, doi: 10.1109/TASC.2022.3162798.

[10] STEAM LEDET, Accessed: Feb. 5, 2024. [Online]. Available: https://cern.ch//ledet

[11] M. Wozniak, E. Schnaubelt, J. Dular, E. Ravaioli, and A. Verweij, "Quench co-simulation of canted cos-theta magnets," *IEEE Trans. Appl. Supercond.*, vol. 34, no. 3, May 2024, Art. no. 4900105, doi: 10.1109/TASC.2023.3338142.

[12] STEAM Framework, Accessed: Feb. 5, 2024. [Online]. Available: https://cern.ch//steam

[13] L. Brouwer et al., "Design and test of a curved superconducting dipole magnet for proton therapy," *Nucl. Instrum. Methods Phys. Res. Sect.: Accel., Spectrometers, Detect. Assoc. Equip.*, vol. 957, Mar. 2020, Art. no. 163414, doi: 10.1016/j.nima.2020.163414.

[14] Y. Tong et al., "Electro-thermal coupling model of quench protection with a quench-back for DCT&CCT superconducting magnets," *IEEE Trans. Appl. Supercond.*, vol. 32, no. 6, Sep. 2022, Art. no. 4701106, doi: 10.1109/TASC.2022.3161254.

[15] R. Kang et al., "A general model for simulating the quench behavior of canted-cosine-theta (CCT) quadrupole magnets," *Cryogenics*, vol. 128, Dec. 2022, Art. no. 103574, doi: 10.1016/j.cryogenics.2022.103574.

[16] Python Programming Language, Accessed: Feb. 5, 2024. [Online]. Available: https://www.python.org/

[17] Gmsh, Accessed: Feb. 5, 2024. [Online]. Available: http://gmsh.info/

[18] C. Geuzaine and J.-F. Remacle, "Gmsh: A 3-D finite element mesh generator with built-in pre- and post- processing facilities," *Int. J. Numer. Methods Eng.*, vol. 79, pp. 1309–1331, May 2009, doi: 10.1002/nme.2579.

[19] GetDP, Accessed: Feb. 5, 2024. [Online]. Available: http://getdp.info/

[20] P. Dular, C. Geuzaine, F. Henrotte, and W. Legros, "A general environment for the treatment of discrete problems and its application to the finite element method," *IEEE Trans. Magn.*, vol. 34, no. 5, pp. 3395–3398, Sep. 1998, doi: 10.1109/20.717799.

[21] Opera Simulation Software. [Online]. Available: https://www.3ds.com/products-services/simulia/products/opera/

[22] *Standard for the Exchange of Product Model Data (STEP)*, Standard ISO-10303-21, ISO, Geneva, Switzerland, Accessed: Feb. 5, 2024. [Online]. Available: https://www.iso.org/standard/63141.html

[23] STEAM Materials Library GitLab Repository, Accessed: Feb. 5, 2024. [Online]. Available: https://gitlab.cern.ch/steam/steam-material-library

[24] S. Wei, "Former Samples (Al 6082-T6) cold test report," CERN, Geneva, Switzerland, Tech. Rep. EDMS 2020, Accessed: Feb. 5, 2024. [Online]. Available: https://edms.cern.ch/document/2381976/1

[25] MATLAB, Accessed: Feb. 5, 2024. [Online]. Available: https://www.mathworks.com/products/matlab.html